Honokiol Induces a Necrotic Cell Death through the Mitochondrial Permeability Transition Pore

Ling Li,[1] Weidong Han,[1] Ying Gu,[4] Shuang Qiu,[2] Qinghua Lu,[1] Jie Jin,[3] Jianhong Luo,[2] and Xun Hu[1]

[1]Cancer Institute, The Second Affiliated Hospital, [2]Department of Neurobiology, and [3]The First Affiliated Hospital, Zhejiang University School of Medicine, Hangzhou, Zhejiang, China; [4]Division of Developmental Biology, Cincinnati Children's Hospital Medical Center, University of Cincinnati, Cincinnati, Ohio

Abstract

Previous reports have shown that honokiol induces apoptosis in numerous cancer cell lines and showed preclinical efficacies against apoptosis-resistant B-cell chronic lymphocytic leukemia and multiple myeloma cells from relapse-refractory patients. Here, we show that honokiol can induce a cell death distinct from apoptosis in HL60, MCF-7, and HEK293 cell lines. The death was characterized by a rapid loss of integrity of plasma membrane without externalization of phosphatidyl serine. The broad caspase inhibitor z-VAD-fmk failed to prevent this cell death. Consistently, caspase activation and DNA laddering were not observed. The death was paralleled by a rapid loss of mitochondrial membrane potential, which was mechanistically associated with the mitochondrial permeability transition pore regulated by cyclophilin D (CypD) based on the following evidence: (*a*) cyclosporin A, an inhibitor of CypD (an essential component of the mitochondrial permeability transition pore), effectively prevented honokiol-induced cell death and loss of mitochondrial membrane potential; (*b*) inhibition of CypD by RNA interference blocked honokiol-induced cell death; (*c*) CypD up-regulated by honokiol was correlated with the death rates in HL60, but not in K562 cells, which underwent apoptosis after being exposed to honokiol. We further showed that honokiol induced a CypD-regulated death in primary human acute myelogenous leukemia cells, overcame Bcl-2 and Bcl-X_L–mediated apoptotic resistance, and was effective against HL60 cells in a pilot *in vivo* study. To the best of our knowledge, this is the first report to document an induction of mitochondrial permeability transition pore–associated cell death by honokiol. [Cancer Res 2007;67(10):4894–903]

Introduction

Cancer drug resistance is a major problem in chemotherapy. The potency of anticancer drugs is largely determined by their efficacies in selectively killing cancer cells and simultaneously inducing drug resistance in cancer cells. Conventional anticancer agents, regardless of their targets and mechanisms, mostly induce apoptosis. Cancer cells are usually sensitive to apoptotic induction initially, but become resistant eventually (1–3). Apoptotic machinery is composed of at least dozens of antiapoptotic and proapoptotic proteins. The balance of antiapoptotic and proapoptotic proteins contributes to the balance of cell growth and cell death. Many lines of evidence have shown an imbalance with elevated antiapoptotic and reduced proapoptotic activities in cancer cells one way or another, including overexpression of antiapoptotic proteins (Bcl-2, Bcl-X_L, Mcl-1, c-FLIP, IAP, and heat shock proteins), mutations of proapoptotic proteins (p53, Apaf-1, Bax, FAS, FADD, and caspase), and loss of caspases (caspase-3 and caspase-8; refs. 4–6). Therefore, besides apoptosis, the other targets which trigger nonapoptotic cell death may compliment defects of the apoptotic machinery (7–10).

Mitochondria plays a central role in cell death. It serves as an integrator of upstream death signaling. Most importantly, mitochondrial outer membrane permeabilization is a committed point in cell death (11, 12). Thus, strategies based on targeting the mitochondrial permeability transition pore, the main mechanism of mitochondrial outer membrane permeabilization by interfering with vital mitochondrial functions, provide us with new opportunities for therapeutic intervention and may help to overcome resistance to standard cancer therapies (11, 13–15). There are several potential pharmacologic targets on the mitochondrial permeability transition pore, such as the voltage-dependent anion channel, the bongkrekic acid–sensitive adenine nucleotide translocase, and cyclophilin D (CypD), which are regarded as key factors in the regulation of mitochondrial permeability transition pore function and cell death (11, 15–19).

Honokiol, a pharmacologically active component present in the traditional Chinese medicinal herb, *Magnolia* species, is of multiple medicinal uses against microbial infection, anxiety, oxidative stress, and platelet aggregation, among others (20, 21). Previous reports have shown the anticancer activities of honokiol. Honokiol induced apoptosis in cancer cell lines, including murine endothelial SVR cells (22), human colorectal carcinoma RKO cells (23), and human squamous lung cancer CH27 cells (24). Honokiol repressed RKO and angiosarcoma growth in nude mice (22, 25). Recently, two important studies showed that honokiol effectively induced caspase-dependent or -independent apoptosis in apoptosis-resistant B-cell chronic lymphocytic leukemia (B-CLL) from B-CLL patients and multiple myeloma (MM) cells from relapse-refractory MM patients. The effective dose of honokiol was not toxic to normal blood cells (26, 27).

In this study, we show that honokiol can induce a CypD-regulated cell death in HL60, MCF-7, HEK293 cell lines, and in primary human acute myelogenous leukemia (AML) cells. This death is distinct from apoptosis and is closely associated with the CypD-dependent mitochondrial permeability transition pore. The capability of inducing cell death through both apoptosis and nonapoptosis makes honokiol a more versatile "killer" of cancer cells.

Note: Supplementary data for this article are available at Cancer Research Online (http://cancerres.aacrjournals.org/).

L. Li, W. Han, and Y. Gu contributed equally to this work.

Requests for reprints: Xun Hu, Cancer Institute, Zhejiang University, 88 Jiefang Road, Hangzhou, Zhejiang, 310009 China. Phone: 86-571-8778-3656; E-mail: huxun@zju.edu.cn.

doi:10.1158/0008-5472.CAN-06-3818

Materials and Methods

Reagents and antibodies. Honokiol was purchased from the National Institute for the Control of Pharmaceutical and Biological Products (Beijing, China) with >99% purity. RPMI 1640, FCS, and 0.25% trypsin were purchased from Life Technologies; reverse transcription-PCR kit was purchased from Promega; staurosporine, vitamin E, butylated hydroxyanisole, cyclosporin A (CsA), bongkrekic acid, *N*-acetyl-L-cysteine, and Hoechst 33342 were purchased from Sigma. The broad-spectrum caspase inhibitor z-VAD-fmk was from Calbiochem. Primary antibodies used were: mouse monoclonal antibodies anti-CypD, anti-Bcl2, and anti-Bcl-X_L (Calbiochem), anti–β-actin (Sigma), anti–caspase-8, and rabbit polyclonal antibodies anti–apoptosis-inducing factor (AIF), anti–caspase-9 (Cell Signaling Technology). The secondary antibodies were FITC or horseradish peroxidase–conjugated anti-rabbit and anti-mouse IgG (Santa Cruz Biotechnology). Plasmid pSFFV-*Neo*, pSFFV-*Bcl-2*, and pSFFV-*Bcl-X_L* were kindly provided by Dr. Steven Grant (Medical College of Virginia, Virginia Commonwealth University, Richmond, VA).

Primary human AML cells. AML patient samples and three normal peripheral blood samples were collected after informed consent and the approval of the hospital's institutional review board. Patients were not receiving therapy at the time of sampling. AML bone marrow specimens with high blast counts (ranging from 75% to 95% as determined by Wright-Giemsa stain), which was supported by immunophenotyping (Supplementary Table S1), were from the Department of Hematology, the First Affiliated Hospital, Zhejiang University School of Medicine. The three normal peripheral blood specimens were acquired from the Blood Bank, Hangzhou, China. Because the patients had high blast counts, enriched AML cell populations containing >95% tumor cells could be prepared using a density gradient separation of samples (Ficoll-Hypaque, Sigma; ref. 28). The mononuclear cells were cultured in RPMI 1640 supplemented with 10% FCS. Normal peripheral blood mononuclear cells (PBMC) were prepared as described above. Viability on samples was >90% as determined by a trypan blue exclusion assay.

Cell cultures and generation of stable cell lines. HL60, MCF-7 cells, or primary AML cells were maintained in RPMI 1640 containing 10% FCS and 300 mg/L of glutamine (Life Technologies), and HEK293 was maintained in DMEM containing 10% FCS and 300 mg/L of glutamine. Cells were grown in a humidified CO_2 incubator at 37°C, and subcultured with 0.25% trypsin 0.02% EDTA. MCF-7/Neo, HEK293/Neo, MCF-7/Bcl-2, HEK293/Bcl-2, MCF-7/Bcl-X_L, and HEK293/Bcl-X_L cells were obtained by transfection with pSFFV-*Neo*, pSFFV-*Bcl-2*, and pSFFV-*Bcl-X_L* cells, respectively, using LipofectAMINE2000 (Invitrogen) according to the manufacturer's instructions. HL60/Neo, HL60/Bcl-2, and HL60/Bcl-X_L cells were derived by transfection of HL60 with pSFFV-*Neo*, pSFFV-*Bcl-2*, and pSFFV-*Bcl-X_L* cells, respectively, via electroporation with a Nucleofection system (Amaxa, Inc.) according to the manufacturer's instructions. After 48 h of transfection, the transfectants were selected in a medium containing 800 μg/mL of G418 (Invitrogen) for 2 to 3 weeks. The colonies were then amplified, the expression of Bcl-2 and Bcl-X_L cells were analyzed by Western blotting.

RNA interference. MCF-7 and HEK293 cells were transfected with either nonspecific or CypD RNA interference (RNAi; final concentration, 100 nmol/L) via LipofectAMINE 2000 according to the manufacturer's instructions (Invitrogen). The cells were then incubated for 96 h prior to Western blot or propidium iodide (PI) exclusion assay. RNAi was introduced into HL60 using a Nucleofection system (Amaxa) according to the manufacturer's instructions. The cells were then incubated for 48 h prior to immunoblot analysis or PI exclusion assay. The RNAi duplex oligo-ribonucleotides were from Invitrogen. The RNA sequences were as follows: (siRNA no. 1) sense, 5′-UUU GAC GUG ACC GAA CAC AAC AUGC-3′; antisense, 5′-GCA UGU UGU GUU CGG UCA CGU CAAA-3′; (siRNA no. 2) sense, 5′-UAG CUC AAC UGG CCACAG UCU GUGA-3′; antisense, 5′-UCA CAG ACU GUG GCC AGU UGA GCUA-3′. BLOCK-iT Fluorescent Oligo (Invitrogen) was used as a quality control to assure the transfection efficiency with Stealth RNAi. Nonspecific RNAi with the same GC content as siRNA nos. 1 and 2 was used as a negative control.

Treatment of cells with honokiol. Unless otherwise stated, throughout this study, HL60 was treated with honokiol at 15 μg/mL for 12 h, MCF-7 and HEK293 were treated with honokiol at 40 μg/mL for 6 h. DMSO (0.1%) was used as vehicle control for all assays.

Apoptosis assays. Apoptotic rates were analyzed by flow cytometry using Annexin V-FITC/PI kit (Sigma) according to the manufacturer's instructions. The procedure was carried out according to the previous reported methods (29). Lower left quadrant, viable cells; lower right quadrant, AV-positive but PI-negative cells (PS externalized apoptotic cells); upper left and right quadrants, necrotic cells. Alternatively, the apoptotic cells were either visually examined for nuclear fragmentation using Hoechst 33342 or detected for hypodiploid percentage using PI as described previously (29, 30).

DNA gel electrophoresis. After treatments, 3×10^6 cells were harvested and washed in PBS. Afterwards, it was processed according to previously reported methods (10).

Measurement of caspase-3/DEVDase activity. Caspase-3 activity was measured using a caspase-3/CPP32 colorimetric assay kit (BioVision Research Products) according to the manufacturer's instructions. Samples were expressed as fold increase on the basal level (DMSO-treated cells).

PI exclusion assay. The loss of integrity of the plasma membrane was determined by PI (Sigma) exclusion assay. After drug treatment, cells were mixed with 30 μg/mL of PI, and dead cells permeable to PI were counted by a fluorescence-activated cell sorter (FACSCalibur, Becton Dickinson).

Immunofluorescent staining of AIF. The procedure was carried out according to previously reported methods (10). After cellular AIF staining, nuclei were stained with PI for 10 min. Samples were examined under an Olympus FV1000 microscope equipped with a 40× oil immersion lens (numerical aperture, 1.2). Images were processed with FV10-ASW software (Olympus). The procedure was carried out at room temperature.

Assessment of permeability transition pore opening by confocal imaging. After drug treatment, 2 to 4×10^4 cells were spun down onto slides, the cells were washed with HBSS and 10 mmol/L of HEPES (HH buffer, pH 7.2) before staining with 1 μmol/L of calcein-AM ester (Molecular Probes) and 5 mmol/L of $CoCl_2$ at room temperature for 15 min. The $CoCl_2$ was added to quench the cytoplasmic fluorescence so that only the calcein-AM fluorescence trapped in the mitochondria was imaged (31, 32). Cells were washed four times and resuspended in HH buffer before being examined under an Olympus FV1000 microscope (Olympus). Images were processed with the FV10-ASW software (Olympus). A band-pass filter of 525 nm was used for capturing the calcein images, and Nomarski optics was used to obtain differential interference contrast images of the cells. To determine the mitochondrial calcein-AM fluorescence levels, individual cells were identified using Nomarski optics and the total mitochondrial fluorescence per cell was measured using Northern Eclipse software, version 5.0.

Reactive oxygen species production and mitochondrial membrane potential. Reactive oxygen species (ROS) and mitochondrial membrane potential (MMP; $\Delta\psi_m$) were measured according to the previous reported methods (31, 32). Briefly, after treatment with honokiol, cells were incubated in RPMI 1640 containing 50 μmol/L of DCFH-DA for 30 min and ROS was scored using a FACSCalibur flow cytometer, and data were analyzed on CellQuest software, version 3.1 (Becton Dickinson). MMP was probed by 5,5′,6,6′-tetrachloro-1,1′,3,3′-tetraethyl-benzimidazolylcarbocyanine iodide (JC-1, a potential-sensitive probe; Molecular Probes) using a FACSCalibur. Briefly, cells were harvested and incubated with medium containing JC-1 (10 μg/mL) for 10 min, washed, and resuspended in 1 mL of PBS for flow cytometry analyses. Controls were done in the presence or absence of 50 μmol/L of fluoro-carbonyl cyanide phenylhydrazone (Merck) for 12 h for MMP or 30% H_2O_2 for 1 h for ROS. In all cases, samples were gated to exclude cellular debris.

Electron microscopy. Treated cells were washed and fixed for 30 min in 2.5% glutaraldehyde. The samples were treated with 1.5% osmium tetroxide, dehydrated with acetone and embedded in Durcupan resin. Thin sections were poststained with lead citrate and examined in the TECNAI 10 electron microscope (Philips, Holland) at 60 kV.

Western blot analysis. The procedure was carried out according to previously reported methods (29). The protein was applied to a 10% to 15% SDS-polyacrylamide gel, transferred to a nitrocellulose membrane, and then

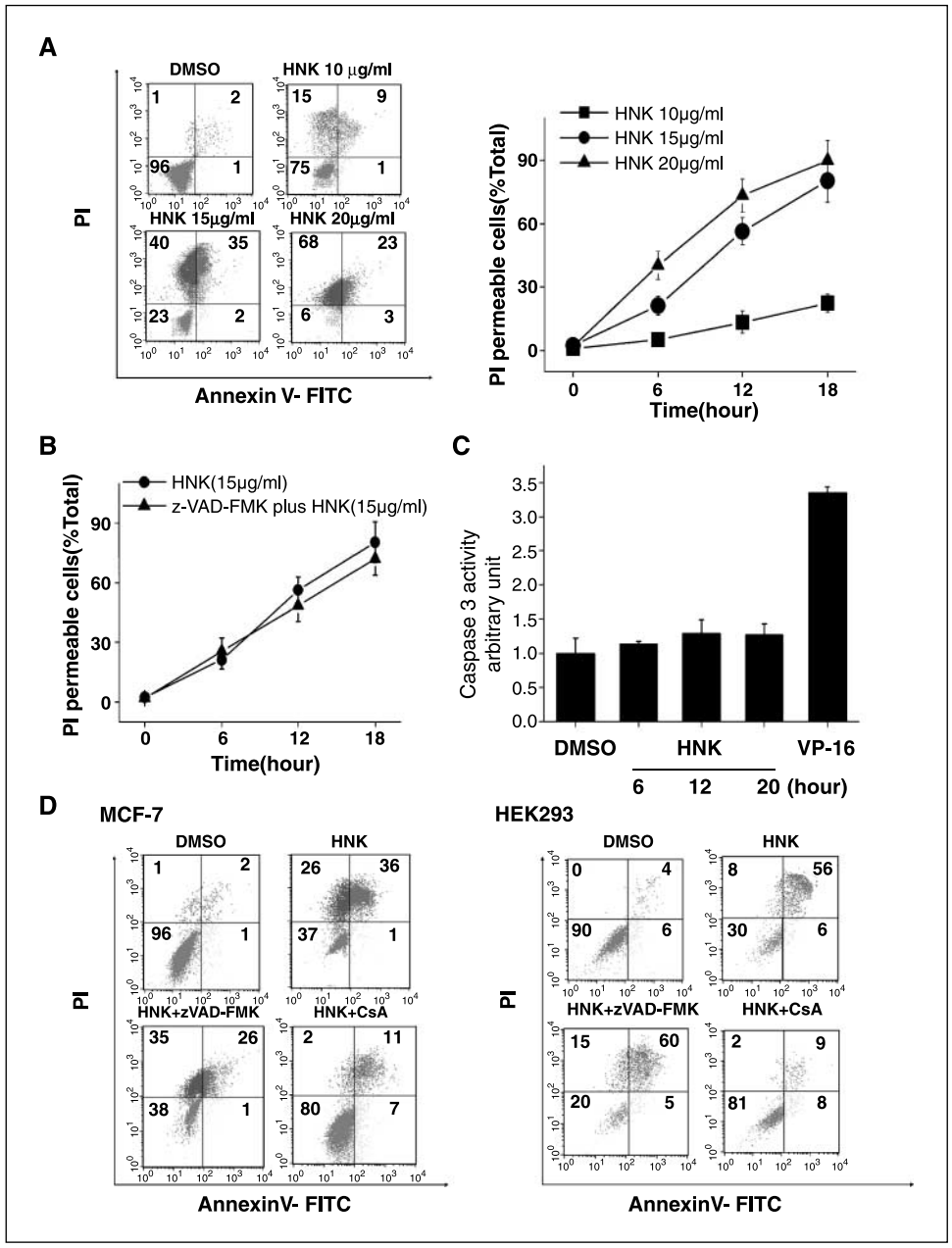

Figure 1. Honokiol induces a cell death without apoptotic characteristics. *A,* HL60 cells were incubated with honokiol (10, 15, and 20 μg/mL) or 0.1% DMSO (vehicle control) for 18 h and assayed for phosphatidyl serine externalization or PI permeability. *B,* HL60 cells were preincubated with or without 50 μmol/L of z-VAD-FMK for 2 h before treatment with honokiol (15 μg/mL) and examined for PI permeability. *C,* HL60 cells were treated with DMSO, honokiol (15 μg/mL) for appropriate intervals, or VP-16 (20 μg/mL for 4 h as positive control), and assayed for caspase-3 activity. *D,* MCF-7 and HEK293 cells were incubated with DMSO or honokiol for 2 h, pretreated with or without 50 μmol/L of z-VAD-FMK or 25 μmol/L of CsA for 2 h, then assayed for phosphatidyl serine externalization as described in Materials and Methods. Results are representative of three individual experiments.

detected by the proper primary and secondary antibodies before visualization with a chemiluminescence kit (Pierce). Visualization was done with a Molecular Imager FX (Bio-Rad Laboratories) using Kodak ID imaging densitometry analysis software on a Macintosh.

Real-time PCR. CypD mRNA was analyzed by quantitative real-time reverse transcription-PCR. After honokiol treatment, cells were collected for total RNA extraction by a TRIzol reagent (Invitrogen) according to the manufacturer's instructions. The quality of the total RNA was confirmed by the integrity of 28S and 18S rRNA. The first-strand cDNA was synthesized from extracted RNA using an Oligo-dT as primer. PCR was done in triplicate in 50 μL reaction volumes using 1.5 μL of cDNA, SYBR Premix Ex Taq containing deoxynucleotide triphosphates (Takara-Bio), 1 μL of carboxy-rhodamine reference dye (1:400 dilution), and 5 pmol of each primer. PCR was done using *CypD* primers (5′-TGGCTAATGCTGGTCCTAAC-3′ and 5′-TGGATGTCCTCCCACTCTTAG-3′) and *β-actin* (5′-TTCCAGCCTTCC-TTCCTGGG-3′ and 5′-TTGCGCTCAGGAGGAGCAAT-3′). Primers for *CypD* spanned exons 5 and 6, and primers for *β-actin* spanned exons 3 and 5. Samples were amplified in a 7700 real-time PCR system (PE Applied Biosystems) for 40 cycles using the following PCR variables: samples were heated at 95°C for 10 s, followed by 40 cycles of amplification of 95°C for 5 s, and 60°C for 30 s. The fluorescent signal was determined using a sequence detector software (PE Applied Biosystems), giving the threshold cycle number (C_T) at which PCR amplification reached a significant threshold. Then the ΔC_T value was defined as the difference of the C_T values between *CypD* and *β-actin*, the internal standard. Accordingly, ΔC_T = (CypD mRNA C_T) − (β-actin mRNA C_T), and the relative CypD mRNA expression level was presented as $2^{-\Delta}C_T$.

PCR was also done in a DNA thermal cycler (Perkin-Elmer) according to previously reported methods (29). The reaction condition used was initial denaturation for 5 min at 95°C followed by 35 cycles of denaturation for 15 s at 95°C, primer annealing for 15 s at 60°C, polymerization for 15 s at 72°C, and final extension for 5 min at 72°C. PCR products were separated on ethidium bromide–stained 1.5% agarose gels. Expected reverse transcription-PCR sizes were 161 bp for *CypD* and 250 bp for *β-actin*.

***In vivo* pilot studies.** To establish a mouse model of human leukemia engrafts, 4-week-old female severe combined immunodeficiency mice

(Shanghai SLAC Laboratory Animal, Co. Ltd.) were inoculated i.p. with 2×10^7 HL60 cells, or were irradiated with 2.0 Gy by a ^{137}Cs gamma-ray source prior to i.v. inoculation with 1×10^7 HL60 cells. Six days after inoculation, animals were grouped randomly and administered i.p. with 100 mg/kg of honokiol or vehicle control suspended in 20% Intralipid (Sino-Swed Pharmaceutical, Corp. Ltd.) with a total volume of 200 μL daily for 6 consecutive days. The survival time of mice was monitored on the daily basis.

Statistical analyses. Unless otherwise stated, data were expressed as the mean ± SD, and analyzed by Student's *t* test.

Results

Honokiol induces cell death with necrotic characteristics. Because the optimal concentrations of honokiol to induce apoptosis in B-CLL and MM cells from patients were ~20 μg/mL (26, 27), and the concentration of honokiol at <10 μg/mL was nontoxic to HL60 cells (33), we treated HL60 cells with honokiol at 10, 15, and 20 μg/mL for 18 h. Unexpectedly, honokiol induced a dominant death characterized by a loss of plasma membrane integrity (PI positivity) but without a significant externalization of phosphatidyl serine (Annexin V-FITC positive; Fig. 1*A*; ref. 34). Consistently, there was neither activation of caspase-3, caspase-8, and caspase-9 (although caspase-3, caspase-8, caspase-9 activation was observed in etoposide–treated cells; Fig. 1*C*; Supplementary Fig. S2*B*), nor was there apoptotic DNA laddering (Supplementary Fig. S1), nor a significant hypodiploid peak (Supplementary Fig. S2*A*). The broad-spectrum caspase inhibitor z-VAD-fmk also failed to prevent honokiol-induced cell death (Fig. 1*B*). These results indicated that caspases were not involved in honokiol-induced HL60 cell death. The similar results of dominant necrotic death or caspase independence (Fig. 1*D*; Supplementary Fig. S2*C*), and the lack of a hypodiploid peak (Supplementary Table S2) were also obtained with MCF-7 and HEK293 treated with honokiol.

Morphologically, honokiol-treated cells did not exhibit apoptotic nuclear fragmentation (Fig. 2). Instead, cells had a necrotic death morphology. In HL60 cells, many rounded mitochondria with damaged internal cisternae were observed, although the inner and outer membranes of the mitochondria seemed to be intact in most cells (Fig. 2*A-c*). There was extensive vacuolation of cytoplasmic organelles and some dense bodies. High-power examination of these structures revealed a heterogeneous mixture of electron-lucent and electron-dense regions, many of which were vacuoles and autophagosomes (Fig. 2*A-d, e*, and *f*). Honokiol-treated MCF-7 and HEK293 cells showed similar necrotic characteristics to HL60 cells (Fig. 2*B*). Taken together, these results indicate that honokiol induced a nonapoptotic death in HL60, MCF-7, and HEK293 cells.

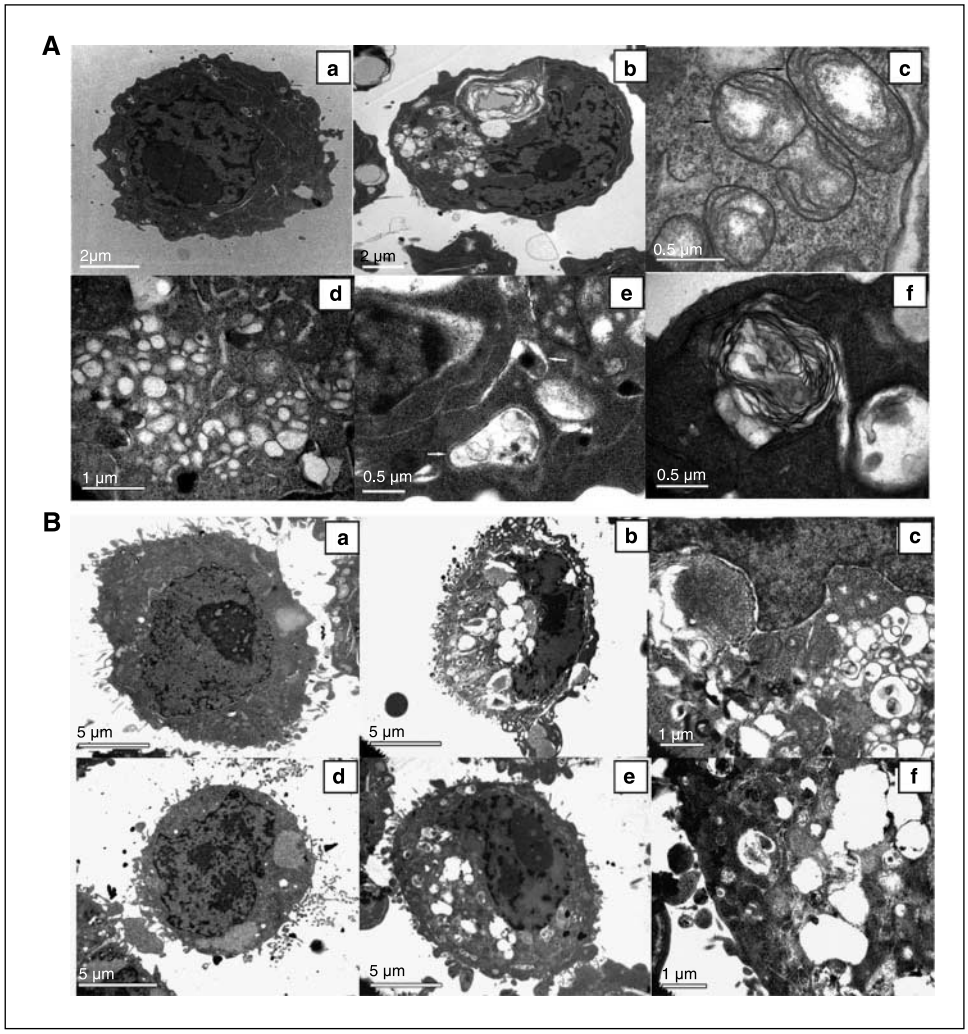

Figure 2. Honokiol induces death with a necrotic morphology. *A, a,* control HL60; *b* to *f,* 15 μg/mL of honokiol-treated cells for 6 h; *b,* main nuclear changes include irregular clumping of chromatin and the appearance of cleared nuclear domains free of chromatin compared with control cells; *c,* high-power magnifications showing rounded mitochondria with disrupted internal structures (*arrows*); *d,* extensive cytoplasmic vacuolation; *e,* autophagosomes (*arrows*); *f,* autophagic vacuoles containing membranous whorls. *Bars,* 2 μm (*a* and *b*), 1 μm (*d*), 0.5 μm (*c, e*, and *f*). *B, a* to *c,* HEK293; *d* to *f,* MCF-7; *a* and *d*, control cells; *b* and *e*, 40 μg/mL of honokiol-treated cells showed a primary and preferential disruption of the cytoplasm architecture after 4 h, whereas the cell nucleus was less affected at the early stages of drug exposure; *c* and *f*, high-power magnifications of honokiol-treated cells. *Bars,* 5 μm (*a, b, d*, and *e*), 1 μm (*c* and *f*). The data are representative of three individual experiments.

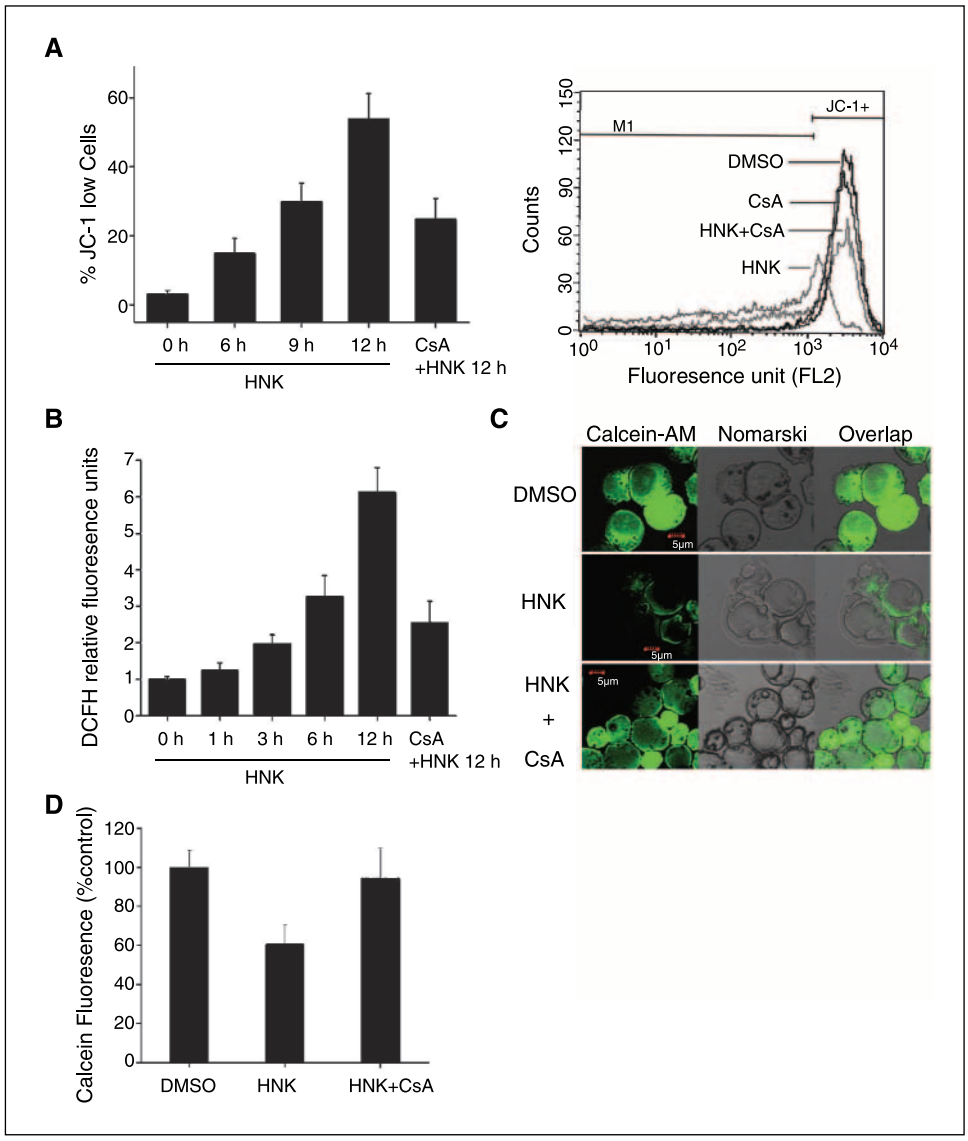

Figure 3. Honokiol-induced death is mechanistically associated with mitochondrial dysfunction. *A,* HL60 cells were incubated with 5 μmol/L of CsA for 2 h prior to treatment with honokiol (15 μg/mL), and assayed for $\Delta\psi_m$. JC-1^{LOW} cells were defined as cells that were gated within the same range as those treated with 50 μmol/L of FCCP which resulted in ~99% of JC-1^{LOW} cells. Representative profiles of JC-1 staining cells (*right*). *B,* cells were treated with honokiol as above and assayed for ROS using DCFH-DA. Cells treated with 30% H_2O_2 were used as a positive control. Relative DCFH fluorescence units were gained from fluorescence mean compared with the control group. *C,* cells pretreated with or without CsA (5 μmol/L) were incubated with honokiol (15 μg/mL) for 6 h and examined for the leakage of mitochondria using calcein-AM in the presence of $CoCl_2$. *D,* quantitation of calcein fluorescence of cells from (*C*) by normalizing mitochondrial calcein fluorescence of 100 treated cells to that of 100 control cells. *Columns,* means from four individual experiments, representative of at least three separate experiments; *bars,* SD.

Honokiol-induced death does not involve a nuclear translocation of AIF. Because honokiol could induce a caspase-independent apoptosis by triggering nuclear translocation of AIF (27), we examined if this protein was involved. As shown in Supplementary Fig. S3*A*, AIF was not translocated to the nuclei in honokiol-treated HL60 cells, although staurosporine-treated cells (a positive control) did have the nuclear localization of AIF.

Honokiol-induced death is associated with a loss of MMP ($\Delta\psi_m$) and an increased production of ROS. Because ultrastructural studies revealed the damaged mitochondria in honokiol-treated cells, we hypothesized that honokiol-induced death was probably due to mitochondrial dysfunction. As shown in Fig. 3*A* and *B*, the loss of $\Delta\psi_m$ was time-dependent and occurred significantly as early as 6 h after honokiol treatment (Fig. 3*A*), accompanied with the production of ROS (Fig. 3*B*).

Honokiol-induced death is associated with the mitochondrial permeability transition pore. Opening of the permeability transition pore may result in dissipation of $\Delta\psi_m$ and respiratory inhibition of ROS production. In another way, prior to the loss of $\Delta\psi_m$, proapoptotic Bcl-2 family members may contribute to the cell death, through action on the mitochondrial outer membrane (35, 36). Because Bcl-2 and Bcl-X_L overexpression (Supplementary Fig. S3*D*) could not inhibit honokiol-induced death in these cells (Supplementary Fig. S3*B* and *C*), the participation of the major Bcl-2 family members in honokiol-induced cell death was largely overruled.

Next, we examined the opening of the mitochondrial permeability transition pore. The status of the permeability transition pore can be determined with the membrane-permeating fluorescent probe calcein-AM, which freely enters but is not able to exit mitochondria except through an open permeability transition pore (31, 32). HL60 cells started to lose mitochondrial calcein-AM fluorescence as early as 4 h after drug exposure, indicating a rapid opening of the permeability transition pore (Fig. 3*C* and *D*).

Honokiol-induced death is associated with CypD. To confirm that the cell death was the result of opening of the permeability transition pore, we examined the effect of permeability transition pore inhibitors on honokiol-induced cell death and mitochondrial damage. CypD, adenine nucleotide translocase, and voltage-dependent anion channels are the major components of the

permeability transition pore (11, 12, 15, 18, 19, 31, 35–38). CsA and bongkrekic acid are two permeability transition pore inhibitors which work by interacting with CypD and adenine nucleotide translocase, respectively. Although CsA could prevent honokiol-induced cell death (Figs. 1*D* and 4*A* and *B*; Supplementary Fig. S5*A*), opening the permeability transition pore, leading to loss of $\Delta\psi_m$ and generation of ROS (Fig. 3), bongkrekic acid did not have inhibitory effects (Supplementary Fig. S5*B*).

To further determine the role of CypD in honokiol-induced cell death, we did RNAi to knock down the endogenous CypD. The BLOCK-iT Fluorescent Oligo was used as a quality control to assure the transfection efficiency, and a nonspecific RNAi (with the same GC content as siRNA nos. 1 and 2) was used as a negative control. In three cell lines, the transfection efficiencies were all >90%. As shown in Fig. 4*C*, 96 h after one single transfection with siRNA no. 1 and siRNA no. 2, CypD was reduced by 85% and 70%, respectively, in MCF-7, and by 75% and 60%, respectively, in HEK293. Forty-eight hours after a single transfection with siRNA no. 1 and siRNA no. 2 by electroporation with the Amaxa system, CypD in HL60 was decreased by 80% and 85%, respectively. Consistently, knockdown of CypD via RNAi significantly prevented honokiol-induced cell death (Fig. 4*D*).

To further elucidate the role of CypD in the process of cell death, we examined the expression of CypD responding to honokiol treatment. The expression of CypD mRNA in HL60, MCF-7, and HEK293 after honokiol treatment was time-dependent. CypD mRNA increased in the early phase and then declined (Fig. 5*A* and *B*). Similar patterns of CypD protein change were also observed (Fig. 5*C* and *D*). The decline of CypD in the later time points was probably a consequence of the cellular and physiologic collapse in the later phase of cell death. In the early phase of cell death, honokiol up-regulated CypD in a dose- and time-dependent manner, which correlated with the death rates in HL60 cells (Supplementary Fig. S4). Interestingly, CypD did not change

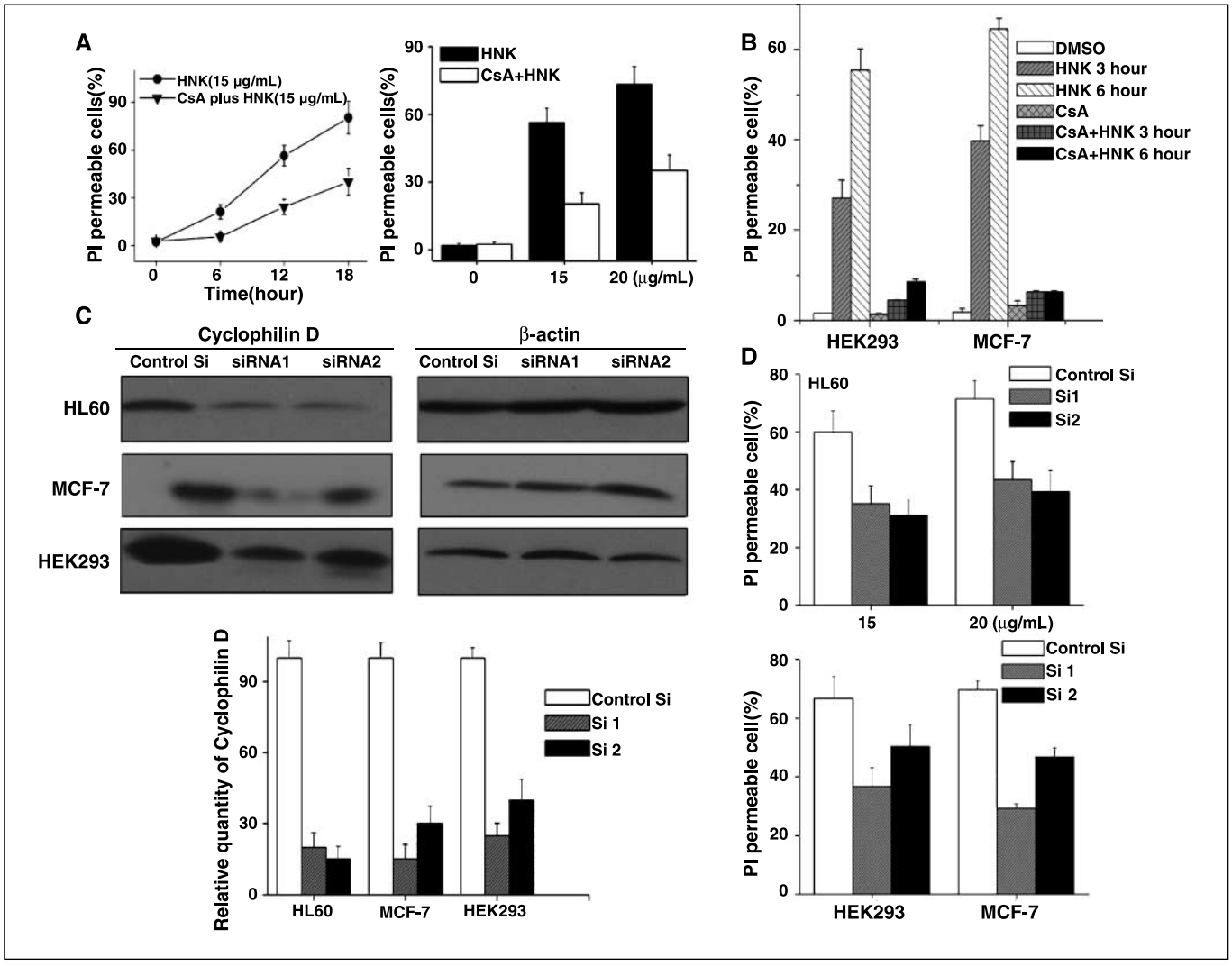

Figure 4. Honokiol-induced death is mechanistically associated with cyclophilin D. *A,* time-dependent (*left*) and concentration-dependent (*right*) PI permeability of HL60 cells treated with honokiol in the presence or absence of CsA (5 μmol/L). *B,* time-dependent PI permeability of MCF-7 or HEK293 cells treated with honokiol (40 μg/mL) in the presence or absence of CsA (25 μmol/L). *C,* CypD knockdown by RNAi measured by a Western blot (*top*) with β-actin as an internal control, which was quantified by a Kodak ID imaging densitometer, and calibrated by an internal standard β-actin. *D,* cells pretreated with control siRNA, siRNA no. 1, and siRNA no. 2 were incubated with honokiol, and assayed for PI permeability. *Columns and points,* means from four individual experiments representative of at least three separate experiments; *bars,* SD.

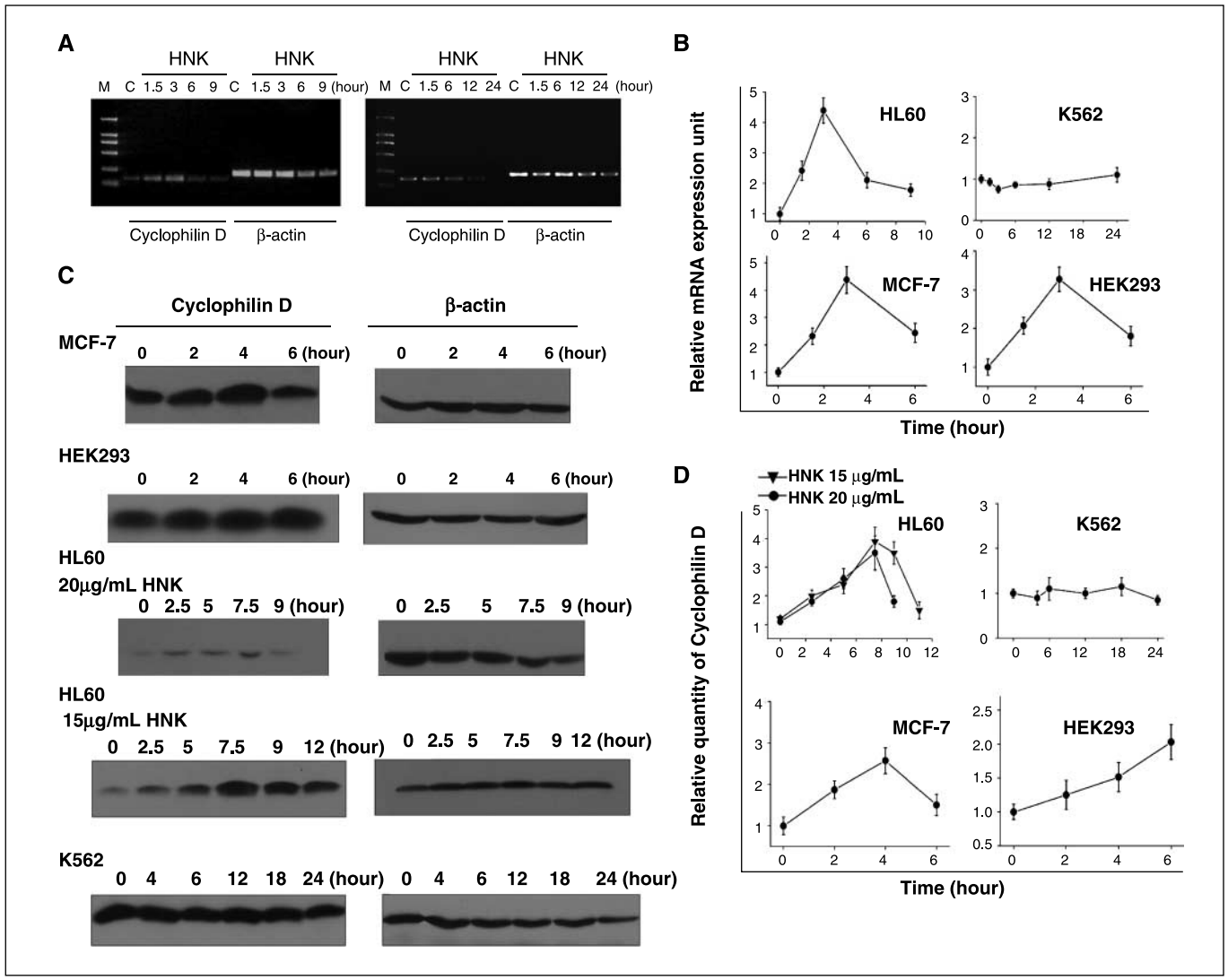

Figure 5. Honokiol-induced death involves a rapid up-regulation of cyclophilin D. *A,* determination of *CypD* in HL60 (*left*) or K562 cells (*right*) treated with 15 μg/mL of honokiol by reverse transcription-PCR with *β-actin* as an internal control. *C,* control; *M,* molecular-weight standard. *B* and *C,* CypD mRNA and protein in honokiol-treated cells for appropriate intervals with β-actin as an internal control, determined by real-time PCR and Western blot as described in Materials and Methods. Honokiol concentrations were: HL60, 15 or 20 μg/mL; K562, 15 μg/mL; MCF-7 or HEK293, 40 μg/mL. *D,* the relative quantity of CypD (*C*). Quantity was processed by a Kodak ID imaging densitometer, and calibrated by the internal standard β-actin. *Points,* means from four individual experiments representative of at least three separate experiments; *bars,* SD.

significantly in K562 cells after honokiol treatment (Fig. 5). Further examination revealed that honokiol induced an apoptosis in K562 cells, which was not prevented by CsA (Supplementary Fig. S6; Supplementary Table S3). The results indicated that the cell death induced by honokiol seemed to be initiated by the up-regulation of CypD, which then triggered the opening of the permeability transition pores, and were consistent with the established evidence that up-regulation of CypD promoted the mitochondrial permeability transition that led to necrosis, whereas knockout of this protein desensitized cells to necrosis (18, 19, 37–41).

Honokiol shows anticancer activities *in vivo.* A prolonged survival time was observed after treatment with honokiol in severe combined immunodeficiency mice inoculated (i.p. or i.v.) with human HL60 cells engrafts. As shown in Fig. 6*D*, in the i.v. group, six vehicle control animals were all dead by day 20 after implantation, in contrast to the first death on day 23 in the honokiol group. The median survival times of the vehicle and honokiol groups were 17 and 29 days, respectively. Similarly, in the i.p. group, five vehicle control animals were all dead by day 30 after implantation, in contrast to the first death on day 33 in the honokiol group. The median survival times of the vehicle and honokiol groups were 24.5 and 37.5 days, respectively.

Effects of honokiol on primary human AML cells. The above results prompted us to investigate if honokiol could also induce a CypD-regulated cell death in primary human AML cells. Among primary cells from a total of 14 patients treated with honokiol, 10 samples underwent a death inhibited by CsA (Table 1). In these samples, honokiol displayed a concentration- and time-dependent killing of AML cells characterized by a loss of plasma membrane integrity (PI positivity) but without a significant externalization of phosphatidyl serine (Annexin V-FITC–positive; Fig. 6*A* and *B*). The death was inhibited by CsA but not z-VAD-fmk (Fig. 6*B*; Table 1).

Honokiol also significantly up-regulated CypD in AML cells such as HL60 cells. The results indicated that the induction of CypD-associated death in human primary AML cells may have potential clinical significance. Honokiol was significantly more toxic toward AML cells than normal PBMCs (Fig. 6*A*; Table 1), agreeable with previous reports (26, 27).

Because honokiol was able to induce either apoptosis or CypD-associated cell death in different types of cells, it was not surprising that honokiol did not exclusively induce CypD-regulated death in AML cells from different individual patients. The mechanisms whereby honokiol induces apoptosis or necrosis would be further addressed in the next section.

Discussion

This study, combined with previous reports, revealed that honokiol could induce different death modes in different cancer cells. Honokiol induced apoptosis in numerous cancer cells (22–24). Phenotypically, honokiol-induced apoptosis could be either caspase-dependent or -independent (26, 27). In the

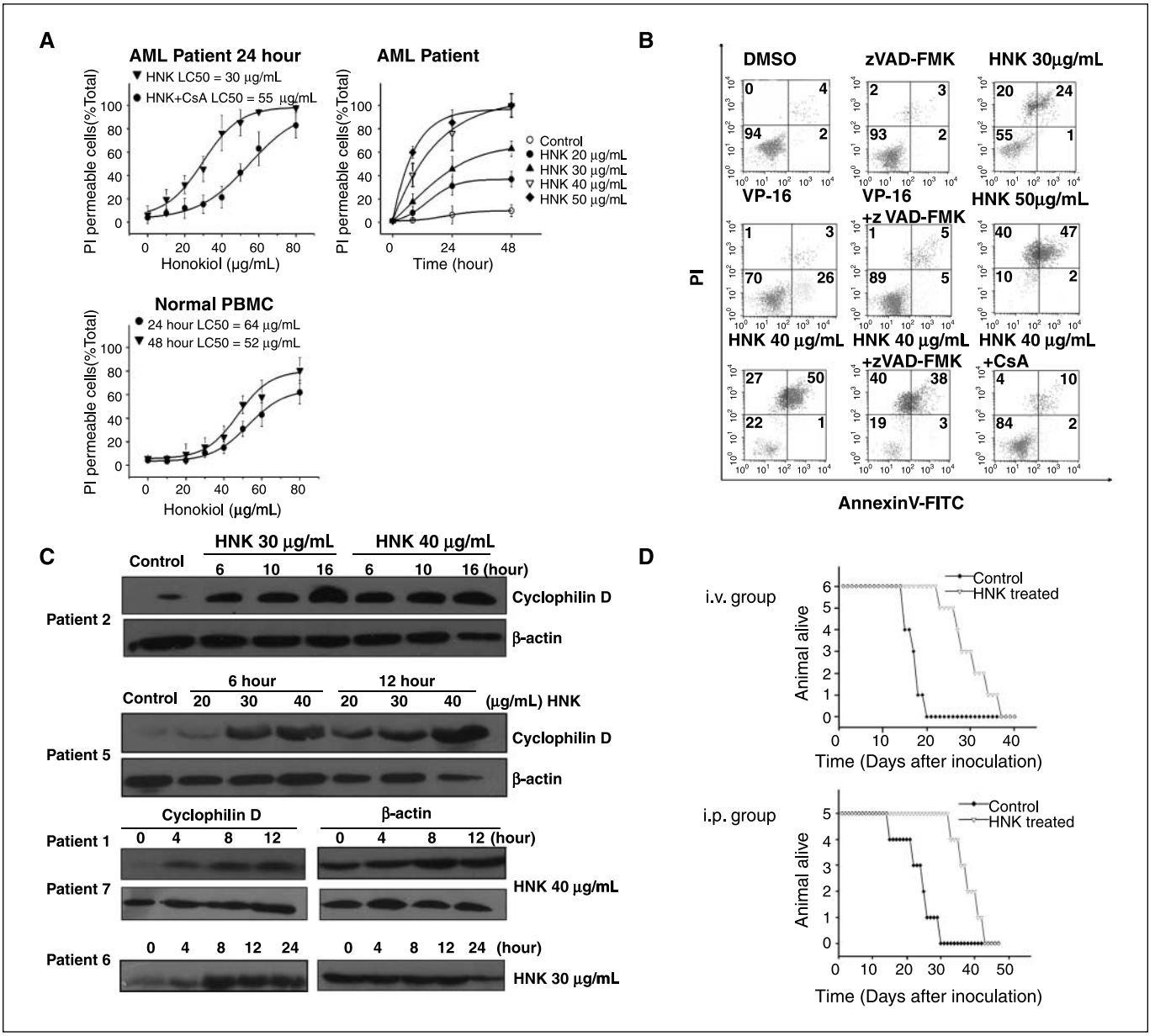

Figure 6. The effects of honokiol on primary human AML cells *in vitro* and HL60 *in vivo*. *A,* mononuclear cells from patients with AML (*top*) were treated with varying concentrations of honokiol in the presence or absence of CsA (5 μmol/L) for the time indicated. Cell death was determined by a PI permeability assay. Data are from patient 2 as a representative. PBMCs from three healthy donors were isolated and treated with varying concentrations of honokiol for 24 and 48 h (*bottom*), and cell death was determined by a PI permeability assay. *B,* mononuclear cells from patients with AML pretreated with or without 50 μmol/L of z-VAD-FMK or 5 μmol/L of CsA for 2 h were treated either with honokiol at the indicated concentrations, or 100 μg/mL of VP-16 (as an apoptosis control), then subjected to apoptosis by Annexin V/PI staining. Data from patient no. 2. *C,* CypD protein level in honokiol-treated AML cells was determined by Western blotting with β-actin as an internal control. Five of 10 representative examples are shown. *D,* survival curves of SCID mice inoculated with HL60. *i.v. group*, HL60 inoculated i.v.; *i.p. group*, HL60 inoculated i.p. *Points,* means from triplicate cultures; *bars,* SD.

Table 1. Characteristics of bone marrow samples from patients with AML

Patient no.	Sex	Age	FAB subtype	Blast counts (%)	LC_{50} of 24-h honokiol / LC_{50} of 24-h honokiol pretreated with CsA (μg/mL)	Dead cells after 24 h, 40 μg/mL honokiol treatment (%)
1 AML	Female	56	M1	85	28/42	83.2 ± 11.9
2 AML	Female	66	M2	85	30/55	76.1 ± 12.0
3 AML	Male	47	M2	80	31/73	70.1 ± 8.1
4 AML	Male	51	M2	74	25/50	90.0 ± 7.9
5 AML	Female	70	M2	80	32/60	70.5 ± 6.3
6 AML	Male	33	M3	92	33/57	74.0 ± 9.6
7 AML	Female	55	M5	89	25/45	81.3 ± 6.9
8 AML	Male	42	M5	68	27/46	67.5 ± 10.1
9 AML	Male	32	M5	94	29/58	67.0 ± 10.8
10 AML	Male	67	M5	73	32/45	69.1 ± 8.2

NOTE: Cells were incubated with or without 5 μmol/L of CsA for 2 h prior to treatment with various concentrations of honokiol for 24 h. Cells were harvested and assayed for PI exclusion as described in Materials and Methods. Data represent means ± SD of three individual experiments.

caspase-independent mode, AIF played a critical role (27). Here, we presented that honokiol induced a cell death in HL60 that was distinct from apoptosis but was closely associated with CypD-regulated mitochondrial permeability transition pore. More importantly, honokiol could induce a similar death to HL60 in primary human AML cells from different individuals, and it was effective against HL60 *in vivo* and against several cancer cell lines overexpressing Bcl-2 and Bcl-X_L. The ability of honokiol to trigger multiple death pathways strongly suggests its effectiveness and versatility in killing cancer cells.

Although the apoptotic or necrotic signaling induced by honokiol is largely unknown, the caspase-dependent and -independent apoptosis triggered by honokiol seemed to be closely related to the regulation of the bcl-2 family members (23, 24, 26, 27), which had been well documented to affect mitochondrial outer membrane permeability (1, 11, 12, 15, 36). In necrotic signaling, honokiol targeted the CypD-regulated mitochondrial permeability transition pore, eventually leading to mitochondrial outer membrane permeability. Therefore, although honokiol could induce different modes of cell death, the death signals by honokiol finally converge in the mitochondria. It is the death signals on the mitochondria that decide between apoptosis or necrosis. If honokiol modulated the Bcl-2 family protein, it would most probably initiate apoptosis because the pore size perforated by dimerization of Bax/Bak allowed the release of cytochrome *c*, AIF, EndoG, and HtrA2/Omi (42). Indeed, the honokiol-triggered apoptotic process involved the up-regulation of proapoptotic members and the down-regulation of antiapoptotic members of the Bcl-2 family, release of mitochondrial cytochrome *c*, activation of caspase, and translocation of AIF (23, 24, 26, 27). If honokiol signaled to permeability transition pore regulated by CypD, it would most probably lead to a nonapoptotic death because the opening of permeability transition pore not only caused a loss of $\Delta\psi_m$ essential for synthesizing ATP, but also accelerated ATP hydrolysis (7, 43). Considering that apoptosis is an ATP-dependent process, depletion of ATP by a massive mitochondrial dysfunction would favor necrosis (7, 43). Although the permeability transition pore would eventually cause the rupture of the mitochondrial outer membrane, and release of apoptotic death effectors, these events could be a downstream consequence of the onset of necrosis. Previous reports have revealed that CypD-related mitochondrial permeability transition led to necrosis, but argue against its involvement in apoptosis (18, 19, 37–41). Consistently, honokiol induced a nonapoptotic death in HL60 featured with a significant up-regulation of CypD, but no observable caspase activation and AIF translocation, and the death was not inhibited by Bcl-2/Bcl-X_L (Supplementary Fig. S3*B–D*). Therefore, the molecular mechanisms whereby honokiol induces cytotoxicity via apoptosis or necrosis are determined by its signals on mitochondria. A similar principle could be extrapolated as to why honokiol did not exclusively induce CypD-associated death in primary AML cells from different individual patients. To date, the signals upstream of mitochondria induced by honokiol are, unfortunately, poorly understood.

Intracellular ROS was elevated after being exposed to honokiol. It has been well documented that besides activating caspase-9, ROS could induce necrosis (44, 45). In some context, intracellular ROS elevation was a downstream consequence of the opening of the permeability transition pore (31, 43, 46). In this study, although antioxidants (vitamin E, butylated hydroxyanisole, and *N*-acetyl-L-cysteine) blocked ROS production (Supplementary Fig. S7*B*), they did not prevent cell death (Supplementary Fig. S7*A*), whereas CsA, a non-antioxidant, effectively prevented cell death (Figs. 1*D* and 4*A* and *B*; Supplementary Fig. S5*A*), strongly suggesting that ROS elevation in HL60 by honokiol was a downstream consequences of the dysfunction of mitochondrial permeability transition pore regulated by CypD.

Honokiol has potential value in clinical applications. Honokiol displayed a satisfactory selectivity between cancer cells (B-CLL, MM, and AML) and normal PBMC (refs. 26, 27; and this study). Our previous pharmacokinetic studies (25) in mice revealed that honokiol was readily absorbed and maintained in the plasma for >10 h. The plasma concentration attainable in mice *in vivo* was 1,000 μg/mL at a dose of 250 mg/kg of honokiol via gastric intubation, significantly exceeding the levels that were toxic to tumor cells *in vitro* (25, 47). The safety of honokiol is indirectly reflected by the facts that Hou-pu, a *Magnolia* species, from which honokiol is extracted, is listed in the Chinese Pharmacopoeia and indexed as a tonic, sedative, and blood-activating and stasis-dissolving prescription, and that Saiboku-to, synonymous with Hou-pu in Japan, has entered clinical trials in Japan for the treatment of asthma (48).

In summary, this study revealed that honokiol induced a death pathway regulated by the mitochondrial permeability transition

pore, in which CypD played a key role. Combined with previous reports, honokiol is a potent anticancer agent which should be examined for further clinical application.

Acknowledgments

Received 10/20/2006; revised 2/8/2007; accepted 3/16/2007.

Grant support: Cheung Kong Scholars Programme (National Ministry of Education, China, and Li Ka Shing Foundation, Hong Kong), a National Ministry of Health China grant (WKJ2006-2-011), and a Bureau for Sciences and Technologies, Zhejiang Province, China grant (2005C23007) to X. Hu.

The costs of publication of this article were defrayed in part by the payment of page charges. This article must therefore be hereby marked *advertisement* in accordance with 18 U.S.C. Section 1734 solely to indicate this fact.

We thank Dr. Steven Grant for the generous gift of plasmid pSFFV-Neo, pSFFV-Bcl-2, and pSFFV-Bcl-X_L, Dr. W. Yang for technical assistance in electroporation, and M. Yang for assistance with the graphics.

References

1. Fulda S, Debatin KM. Extrinsic versus intrinsic apoptosis pathways in anticancer chemotherapy. Oncogene 2006;25:4798–811.
2. Pommier Y, Sordet O, Antony S, Hayward RL, Kohn KW. Apoptosis defects and chemotherapy resistance: molecular interaction maps and networks. Oncogene 2004;23:2934–49.
3. Bremer E, van Dam G, Kroesen BJ, de Leij L, Helfrich W. Targeted induction of apoptosis for cancer therapy: current progress and prospects. Trends Mol Med 2006; 12:382–93.
4. Certo M, Moore V, Nishino M, et al. Mitochondria primed by death signals determine cellular addiction to antiapoptotic BCL-2 family members. Cancer Cell 2006; 9:351–65.
5. Mashima T, Tsuruo T. Defects of the apoptotic pathway as therapeutic target against cancer. Drug Resist Updat 2005;8:339–43.
6. Kim R, Emi M, Tanabe K, Murakami S, Uchida Y, Arihiro K. Regulation and interplay of apoptotic and non-apoptotic cell death. J Pathol 2006;208:319–26.
7. Zong WX, Thompson CB. Necrotic death as a cell fate. Genes Dev 2006;20:1–15.
8. Janmaat ML, Rodriguez JA, Jimeno J, Kruyt FA, Giaccone G. Kahalalide F induces necrosis-like cell death that involves depletion of ErbB3 and inhibition of Akt signaling. Mol Pharmacol 2005;68:502–10.
9. Broker LE, Huisman C, Ferreira CG, Rodriguez JA, Kruyt FA, Giaccone G. Late activation of apoptotic pathways plays a negligible role in mediating the cytotoxic effects of discodermolide and epothilone B in non-small cell lung cancer cells. Cancer Res 2002;62: 4081–8.
10. Okada M, Adachi S, Imai T, et al. A novel mechanism for imatinib mesylate-induced cell death of BCR-ABL-positive human leukemic cells: caspase-independent, necrosis-like programmed cell death mediated by serine protease activity. Blood 2004;103:2299–307.
11. Fantin VR, Leder P. Mitochondriotoxic compounds for cancer therapy. Oncogene 2006;25:4787–97.
12. Kroemer G. Introduction: mitochondrial control of apoptosis. Biochimie 2002;84:103–4.
13. Chernyak BV, Bernardi P. The mitochondrial permeability transition pore is modulated by oxidative agents through both pyridine nucleotides and glutathione at two separate sites. Eur J Biochem 1996;238:623–30.
14. Stadtman ER. Protein oxidation in aging and age-related diseases. Ann N Y Acad Sci 2001;928:22–38.
15. Zamzami N, Larochette N, Kroemer G. Mitochondrial permeability transition in apoptosis and necrosis. Cell Death Differ 2005;12 Suppl 2:1478–80.
16. Zaid H, Abu-Hamad S, Israelson A, Nathan I, Shoshan-Barmatz V. The voltage-dependent anion channel-1 modulates apoptotic cell death. Cell Death Differ 2005;12:751–60.
17. Belzacq AS, El Hamel C, Vieira HL. Adenine nucleotide translocator mediates the mitochondrial membrane permeabilization induced by lonidamine, arsenite and CD437. Oncogene 2001;20:7579–87.
18. Nakagawa T, Shimizu S, Watanabe T, et al. Cyclophilin D-dependent mitochondrial permeability transition regulates some necrotic but not apoptotic cell death. Nature 2005;434:652–8.
19. Baines CP, Kaiser RA, Purcell NH, et al. Loss of cyclophilin D reveals a critical role for mitochondrial permeability transition in cell death. Nature 2005;434: 658–62.
20. Li TSC. Chinese and related North American herbs: phytopharmacology and therapeutic values. Boca Raton (FL): CRC Press; 2002.
21. Liou KT, Shen YC, Chen CF, Tsao CM, Tsai SK. Honokiol protects rat brain from focal cerebral ischemia-reperfusion injury by inhibiting neutrophil infiltration and reactive oxygen species production. Brain Res 2003;992:159–66.
22. Bai X, Cerimele F, Ushio-Fukai M, et al. Honokiol, a small molecular weight natural product, inhibits angiogenesis *in vitro* and tumor growth *in vivo*. J Biol Chem 2003;278:35501–7.
23. Wang T, Chen F, Chen Z, et al. Honokiol induces apoptosis through p53-independent pathway in human colorectal cell line RKO. World J Gastroenterol 2004;10: 2205–8.
24. Yang SE, Hsieh MT, Tsai TH, Hsu SL. Downmodulation of Bcl-XL, release of cytochrome *c* and sequential activation of caspases during honokiol-induced apoptosis in human squamous lung cancer CH27 cells. Biochem Pharmacol 2002;63:1641–51.
25. Chen F, Wang T, Wu YF, et al. Honokiol: a potent chemotherapy candidate for human colorectal carcinoma. World J Gastroenterol 2004;10:3459–63.
26. Battle TE, Arbiser J, Frank DA. The natural product honokiol induces caspase-dependent apoptosis in B-cell chronic lymphocytic leukemia (B-CLL) cells. Blood 2005; 106:690–7.
27. Ishitsuka K, Hideshima T, Hamasaki M, et al. Honokiol overcomes conventional drug resistance in human multiple myeloma by induction of caspase-dependent and -independent apoptosis. Blood 2005;106: 1794–800.
28. Bruserud Ø, Gjertsen BT, Foss B, Huang TS. New strategies in the treatment of acute myelogenous leukemia (AML): *in vitro* culture of aml cells—the present use in experimental studies and the possible importance for future therapeutic approaches. Stem Cells 2001;19:1–11.
29. Li L, Lu Q, Shen Y, Hu X. Schisandrin B enhances doxorubicin-induced apoptosis of cancer cells but not normal cells. Biochem Pharmacol 2006;71:584–95.
30. Nakahara C, Nakamura K, Yamanaka N, et al. Cyclosporin-A enhances docetaxel-induced apoptosis through inhibition of nuclear factor-κB activation in human gastric carcinoma cells. Clin Cancer Res 2003;9: 5409–16.
31. Vande Velde C, Cizeau J, Dubik D, et al. BNIP3 and genetic control of necrosis-like cell death through the mitochondrial permeability transition pore. Mol Cell Biol 2000;20:5454–68.
32. Bernardi P, Scorrano L, Colonna R, Petronilli V, Di Lisa F. Mitochondria and cell death: mechanistic aspects and methodological issues. Eur J Biochem 1999;264:687–701.
33. Fong WF, Tse AK, Poon KH, Wang C. Magnolol and honokiol enhance HL-60 human leukemia cell differentiation induced by 1,25-dihydroxyvitamin D3 and retinoic acid. Int J Biochem Cell Biol 2005;37: 427–41.
34. Vermes I, Haanen C, Steffens-Nakken H, Reutelingsperger C. A novel assay for apoptosis, flow cytometric detection of phosphatidylserine expression on early apoptotic cells using fluorescein labelled Annexin V. J Immunol Methods 1995;184:39–51.
35. Martinou JC, Green DR. Breaking the mitochondrial barrier. Nat Rev Mol Cell Biol 2001;2:63–7.
36. Green DR, Kroemer G. The pathophysiology of mitochondrial cell death. Science 2004;305:626–9.
37. Halestrap A. Biochemistry: a pore way to die. Nature 2005;434:578–9.
38. Schneider MD. Cyclophilin D: knocking on death's door. Sci STKE 2005;287:pe26.
39. Schinzel AC, Takeuchi O, Huang Z, et al. Cyclophilin D is a component of mitochondrial permeability transition and mediates neuronal cell death after focal cerebral ischemia. Proc Natl Acad Sci U S A 2005;102: 12005–10.
40. Basso E, Fante L, Fowlkes J, Petronilli V, Forte MA, Bernardi P. Properties of the permeability transition pore in mitochondria devoid of cyclophilin D. J Biol Chem 2005;280:18558–61.
41. Li Y, Johnson N, Capano M, Edwards M, Crompton M. Cyclophilin-D promotes the mitochondrial permeability transition but has opposite effects on apoptosis and necrosis. Biochem J 2004;383:101–9.
42. Cande C, Vahsen N, Garrido C, Kroemer G. Apoptosis-inducing factor (AIF): caspase-independent after all. Cell Death Differ 2004;11:591–5.
43. Crompton M. The mitochondrial permeability transition pore and its role in cell death. Biochem J 1999;341: 233–49.
44. Yu SW, Wang H, Poitras MF, et al. Mediation of poly(ADP-ribose) polymerase-1-dependent cell death by apoptosis-inducing factor. Science 2002;297:259–63.
45. Waring P. Redox active calcium ion channels and cell death. Arch Biochem Biophys 2005;434:33–42.
46. Kroemer G, Zamzami N, Susin SA. Mitochondrial control of apoptosis. Immunol Today 1997;18:44–51.
47. Tsai TH, Chou CJ, Cheng FC, Chen CF. Pharmacokinetics of honokiol after intravenous administration in rats assessed using high-performance liquid chromatography. J Chromatogr B Biomed Appl 1994; 655:41–5.
48. Egashira Y, Nagano H. A multicenter clinical trial of TJ-96 in patients with steroid-dependent bronchial asthma. A comparison of groups allocated by the envelope method. Ann N Y Acad Sci 1993;685:580–3.